

NASA Technical Memorandum 105940
AIAA-93-0021

IN-25
136519
P.11

Simplified Jet-A Kinetic Mechanism for Combustor Application

Chi-Ming Lee and Krishna Kundu
*Lewis Research Center
Cleveland, Ohio*

and

Bahman Ghorashi
*Cleveland State University
Cleveland, Ohio*

Prepared for the
31st Aerospace Sciences Meeting
sponsored by the American Institute of Aeronautics and Astronautics
Reno, Nevada, January 11-14, 1993

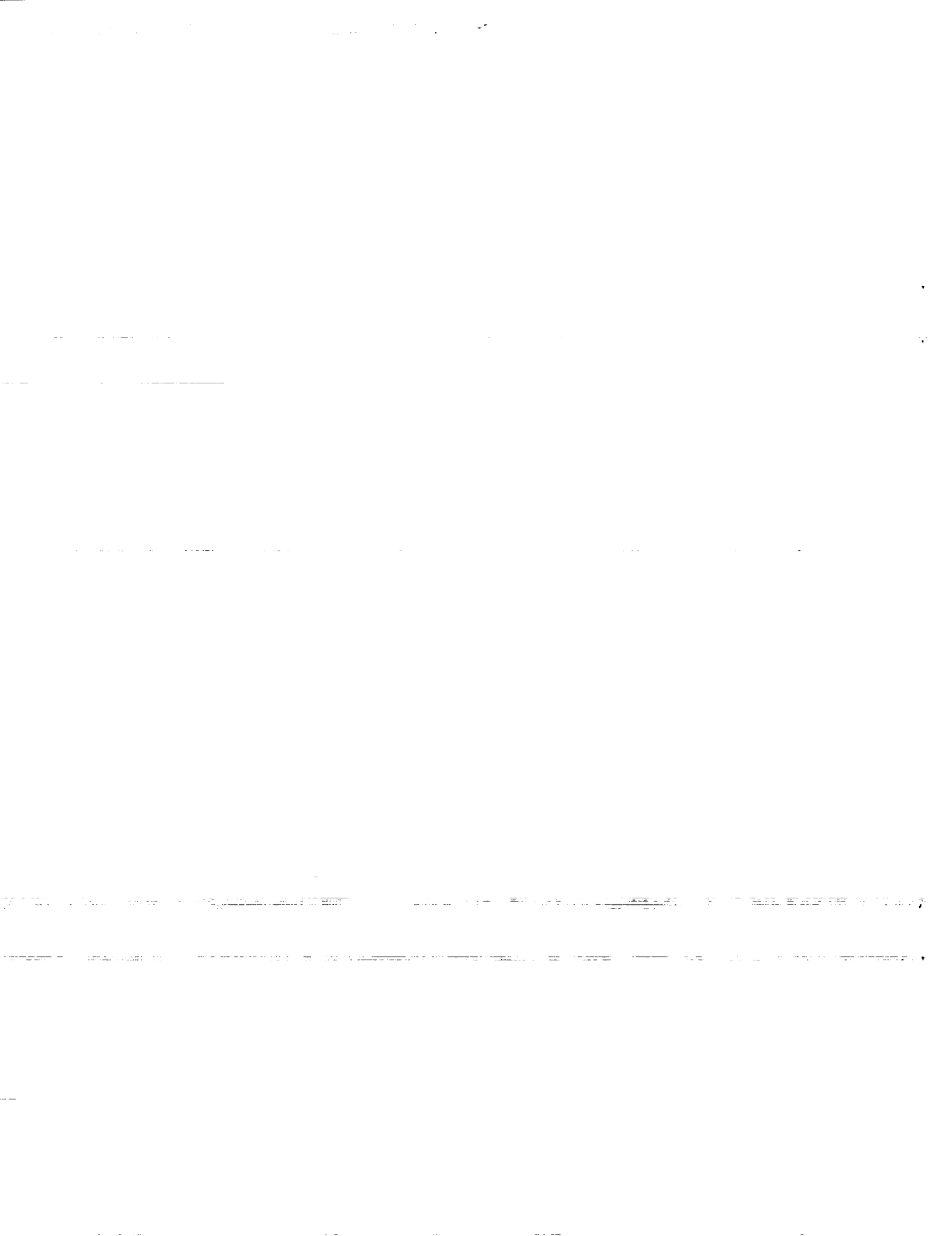
(NASA-TM-105940) SIMPLIFIED JET-A
KINETIC MECHANISM FOR COMBUSTOR
APPLICATION (NASA) 11 p

N93-15504

Unclass

NASA

63/25 0136519



SIMPLIFIED JET FUEL REACTION MECHANISM FOR LEAN BURN COMBUSTION APPLICATION

Chi-Ming Lee and Krishna Kundu
National Aeronautics and Space Administration
Lewis Research Center
Cleveland, Ohio 44135

and

Bahman Ghorashi
Cleveland State University
Cleveland, Ohio 44115

Abstract

Successful modeling of combustion and emissions in gas turbine engine combustors requires an adequate description of the reaction mechanism. For hydrocarbon oxidation, detailed mechanisms are only available for the simplest types of hydrocarbons such as methane, ethane, acetylene, and propane.^{1,2} These detailed mechanisms contain a large number of chemical species participating simultaneously in many elementary kinetic steps. Current computational fluid dynamic (CFD) models must include fuel vaporization, fuel-air mixing, chemical reactions, and complicated boundary geometries.

To simulate these conditions a very sophisticated computer model is required, which requires large computer memory capacity and long run times. Therefore, gas turbine combustion modeling has frequently been simplified by using global reaction mechanisms, which can predict only the quantities of interest: heat release rates, flame temperature, and emissions.

Jet fuels are wide-boiling-range hydrocarbons with ranges extending through those of gasoline and kerosene. These fuels are chemically complex, often containing more than 300 components. Jet fuel typically can be characterized as containing 75 vol % paraffin compounds and 25 vol % aromatic compounds. A five-step Jet-A fuel mechanism which involves pyrolysis and subsequent oxidation of paraffin and aromatic compounds is presented here. This mechanism is verified by comparing with Jet-A fuel ignition delay time experimental data, and species concentrations obtained from flametube experiments. This five-step mechanism appears to be better than the current one- and two-step mechanisms.

Introduction

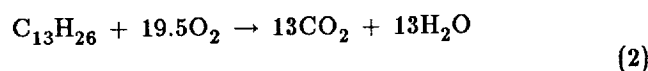
Jet fuel oxidation involves a very large number of reaction species, thus a large number of differential equations are required to develop an acceptable kinetic

mechanism. These differential equations are usually stiff and require special integration techniques. In addition, the specific rate constants of the elementary reactions either are not available in the literature, or are not necessarily well known and can be a potential source of error. The present kinetic mechanisms attempt to simplify the chemistry in order to predict quantities of interest, such as heat release rates, flame temperature, and concentration of important principal species such as unburned hydrocarbons, CO, and CO₂.

The simplified Jet-A chemical kinetics mechanism is based on the modified Arrhenius equation,

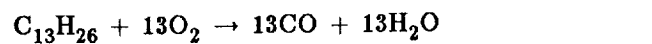
$$k = AT^n \exp(-E/RT) \quad (1)$$

where the rate k depends on the temperature T , temperature exponent n , an activation energy E , and a pre-exponential collision frequency factor A . The simplest Jet-A reaction mechanism is the one-step mechanism:

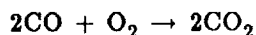


$$\frac{A}{7.5 \times 10^{10}} \quad \frac{n}{0} \quad \frac{E(\text{Kcal/kg mol})}{41\ 000}$$

The activation energy E value of 41 000 Kcal/kg mol has been reported by Freeman and Lefebvre³ for kerosene fuel. The collision frequency factor A value of 7.5×10^{10} has been determined by comparison with Jet-A fuel ignition delay time data. A slightly more complex mechanism is the two-step mechanism, which is very similar to what was proposed by Edelman and Fortune:⁴



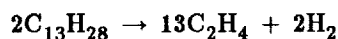
$$\frac{A}{3.37 \times 10^{11}} \quad \frac{n}{0} \quad \frac{E(\text{Kcal/kg mol})}{41\ 000}$$



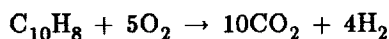
$$\frac{A}{3.48 \times 10^{11}} \frac{n}{2} \frac{E(\text{Kcal/kg mol})}{20 \ 140} \quad (4)$$

The rate expression for the reaction (Eq. 4) is reported by Hautman and Dryer.⁵ The collision frequency factor of 3.37×10^{11} for reaction (Eq. 3) has been determined by comparison with Jet-A fuel ignition delay time data. However, neither of these mechanisms account for molecular hydrogen, and the predicted flame temperatures are higher than experimental results.

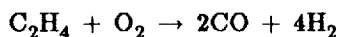
The proposed Jet-A fuel kinetic mechanism is represented by a five-step mechanism listed below. Initially the paraffin base hydrocarbon molecule is broken down into hydrocarbon fragments.⁶ For simplicity, only one major hydrocarbon $\text{C}_{13}\text{H}_{28}$ will be tracked in this mechanism.



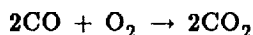
$$\frac{A}{8.0 \times 10^{10}} \frac{n}{0} \frac{E(\text{Kcal/kg mol})}{41 \ 000} \quad (5)$$



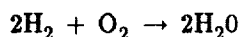
$$\frac{A}{2.4 \times 10^{11}} \frac{n}{0} \frac{E(\text{Kcal/kg mol})}{41 \ 000} \quad (6)$$



$$\frac{A}{2.2 \times 10^9} \frac{n}{2} \frac{E(\text{Kcal/kg mol})}{28 \ 600} \quad (7)$$



$$\frac{A}{3.48 \times 10^{11}} \frac{n}{2} \frac{E(\text{Kcal/kg mol})}{20 \ 140} \quad (8)$$



$$\frac{A}{3.0 \times 10^{20}} \frac{n}{-1} \frac{E(\text{Kcal/kg mol})}{0} \quad (9)$$

The rate expressions for the overall reactions (Eqs. (7) to (9)) are reported by Hautman and Dryer.⁵ Reaction (5) is the overall paraffin compound pyrolysis step, and reaction (6) is the overall aromatic compound oxidation step. The value of the activation energy, E , of 41 000 Kcal/kg mol is reported by Freeman and

Lefebvre for kerosene fuel. The values of collision frequency factor of 8.0×10^{10} for reaction (5), and 2.4×10^{11} for reaction (6) are determined by comparison with Jet-A fuel ignition delay time data. The full mechanism is based on the standard mechanism of Miller and Bowman⁸ coupled with Eqs. (5) and (6). This mechanism involves 51 species and 242 reactions and requires significant computer resources, demonstrating the need for a reduced kinetic mechanism for engineering calculations.

Extensive measurements of species concentrations have been obtained from high pressure, high temperature flow reactor experiments. These data provided insight for the development of a new kinetic mechanism for jet-A fuel oxidation.

Experimental Apparatus and Procedure

Test Facility

The flametube combustor is mounted in the CE5B test facility, which is located in the Engine Research Building (Bldg. 5) at NASA Lewis Research Center. Tests were conducted with combustion inlet air pressure ranging from 10 to 15 atm (147 to 221 psia). A natural gas preheater is used to supply nonvitiated air at 755 to 866 K (900 to 1100 °F) inlet temperature. The temperature of the air is controlled by mixing the heated air with cold bypass air. Downstream of the combustor rig, quench water is sprayed into the gas stream to cool the exhaust to below 333 K (140 °F). Total pressure of the combustor, and airflow through the heat exchanger and bypass flow system are regulated by remotely controlled valves.

The fuel used for this work is specified by the ASTM Jet-A turbine fuel designation. This is a multicomponent kerosene-type fuel commonly used in gas turbine engines. Ambient temperature Jet-A, with a hydrocarbon ratio of 1.96, is supplied to the fuel injector. Flow rates are measured with a calibrated turbine flow meter and were varied from 0.1 to 4.0 GPM with a supply pressure of 650 psig.

Test Rig

The high pressure and temperature test rig used in this experiment consists of an inlet section, fuel injection and vaporization section, flameholder, and combustion section. The combustor test rig is illustrated schematically in Fig. 1. The test section is square having an area of 58 cm² (9 in.²). A square cross-sectional flametube was chosen based on the need to incorporate windows for nonintrusive diagnostic measurements. The

premixed/prevaporization section, and the combustion section are 27 cm (10.5 in.) and 74 cm (29 in.) long, respectively. A ceramic refractory material is used as a liner in the combustion section. This insulating material enables the reactor to be characterized as a one-dimensional adiabatic plug flow reactor.

Fuel Injector

Jet-A fuel is introduced into the airstream by means of a multiple-pass passage fuel injector shown in Fig. 2. The fuel injector was designed to provide good dispersion of fuel in the airstream by injecting equal quantities of fuel into each of the individual passages. The injector used in these tests has 16 square passages. Each passage was machined to form a converging/diverging flowpath. The 64-percent blockage helps to insure a uniform velocity profile over the entire flowfield. The pressure drop across the injector ranges between 3 and 6 percent of the inlet pressure.

Flameholder

A 1.27 cm (0.50 in.) thick perforated plate flameholder, was made from Inconel 718, and is shown in Fig. 3. The plate, used to stabilize the flame, contains a staggered array of 36 holes, 0.64 cm (0.25 in.) in diameter, which results in a flow blockage of 80 percent. The holes have a smooth inlet radius on the upstream side of the plate, and a thermal barrier coating (ZrO) on the downstream side of the plate for extended thermal wear. The total pressure drop across the flameholder ranged from 5 to 12 percent of inlet air pressure.

Combustion Section

The water-cooled combustion section has a square cross-sectional area of 58 cm² (9 in.²), and is 74 cm (29 in.) long. A sketch of the cross section is shown in Fig. 4. For the inlet conditions listed above, adiabatic flame temperatures ranging from 1700 to 2089 K (2600 to 3300 °F) were measured in the combustor section. The flowpath is lined with a high temperature castable refractory material to minimize the heat loss. A high temperature, insulating, ceramic fiber paper is placed between the refractory material and the stainless steel water-cooled housing. The paper serves two purposes: (1) to reduce the heat loss and minimize cold-wall effects; and (2) to compensate for the difference in thermal expansion between the ceramic and the housing. The stainless steel housing is water-cooled through copper tubing coils wrapped and welded to its outer diameter.

Instrumentation

The combustion gases are sampled with six water-cooled sampling probes located 10.2, 30.5, and 50.8 cm (4, 12, and 20 in.) downstream of the flameholder, as seen in Fig. 2. There are two probes at each axial location, with the top probes positioned 1.57 cm (0.62 in.) to the left of center (when looking downstream), and the bottom probes positioned the same distance to the right of center. The probes are 1.57 cm (0.62 in.) in diameter with five 1.02 mm (0.040 in.) I.D. sampling tubes manifolded together and terminating 1.51 cm (0.594 in.) apart along the probe length. Steam-traced stainless steel tubing, 6.4 mm (0.25 in.) O.D. and approximately 15.2 m (50 ft) in length, connect the gas sample probes to the gas analysis equipment. The steam tracing prevents the condensation of unburned hydrocarbons in the line. The probes are mounted on pneumatically operated cylinders interconnected with remotely operated solenoid valves, which allows two probe positions: in and out. The analysis of sample gas was performed by inserting only one probe into the combustion zone at a time, thus minimizing flow disturbances which could affect rig operation.

In addition to gas analysis, pressure and temperatures are measured along the test rig. At the exit of the inlet plenum, a rake containing five total pressure probes and a wall static tap are used to determine the air velocity profile. The inlet temperature is measured with two chromel/alumel thermocouples. Pressure and temperature are also measured upstream of the flameholder to determine the presence of upstream burning and the fuel injector pressure drop. The adiabatic flame temperature in the combustion section is measured using two platinum/rhodium thermocouples located 40.6 cm (16 in.) and 58.4 cm (23 in.) downstream of the flameholder. A pressure tap at the exit of the combustor is used to calculate the pressure drop across the flameholder and the combustion section.

Validation of Mechanism

The experimental Jet-A oxidation results for this study were obtained using a flametube reactor. The flametube has a 3-in. by 3-in. test section, insulated by 2 in. of ceramic material. The experiments conducted were intended to be spatially homogeneous, so that radial transport effects may be neglected. Vaporization of injected liquid Jet-A fuel and mixing of the vaporized fuel with air was completed upstream of the flameholder.

Since inlet conditions control the degree of vaporization and mixing, they must be chosen carefully. In this study, an inlet temperature (T_{in}) of 1000 °F and inlet pressure (P_{in}) of 10 atm was chosen to assure total vaporization for equivalence ratios less than 0.6. The equivalence ratio was varied from 0.40 to 0.60. Recently, Lai⁹ used a Phase Doppler Particle Analyzer to measure a mean droplet size of 40 μm for the fuel injector used in this study. Deur¹⁰ then applied the KIVA-II code and predicted 100 percent vaporization before the fuel injector exit (Fig. 5) at $T_{in} = 1025$ °F, $P_{in} = 142$ psi, equivalence of 0.60, and $SMD = 40$ μm .

To study the fuel-air mixing effectiveness, a focused Schlieren technique has been used¹¹. This provided a time-history of the flowfield at rates up to 10 000 frames/sec, using a high speed camera. Images from frames of the high speed film were digitized and color-enhanced to reveal regions of various density gradients (Fig. 6).

A method of extracting quantitative information from this type of image was devised. As shown in Fig. 6, if vertical lines are drawn at different axial stations in the flow, the degree of mixing as the flow proceeds downstream can be compared. Along each line, the mean and standard deviation of the image pixel intensities is found. A relatively low standard deviation is produced when there is little change in density gradients along the line. When a line cuts across a region of intense mixing, a higher standard deviation is found, as seen for example in lines D, E, and F. As the mixing is completed, line I crosses a more uniform flowfield and its standard deviation is lower. This method can be used to quantitatively compare degree of mixedness at various axial locations.

From these studies, the fuel-air mixture in the premixing section of the flametube was found to be pre-vaporized and premixed. The inlet fuel-air mixture velocity was constrained by requiring combustion to be stabilized, but still sufficient to result in turbulent conditions. The combustion wall was insulated, and the amount of Jet-A injected was less than 1 percent on a molar basis. Thus, the flametube reactor was characterized as one-dimensional plug flow reactor.

Results

Four mechanisms were examined, they are: one-step, two-step, five-step, and full mechanisms. These four mechanisms were then integrated into the LSENS code¹² to perform case studies. Results from these case studies are shown in Figs. 7 to 10. Jet-A fuel ignition delay times (Fig. 7), flame temperatures (Fig. 8), and species concentrations (Figs. 9 and 10) for various equivalence

ratios have been calculated. The calculated results from the full mechanism shows excellent agreement with experimental data as expected. The five-step mechanism produced reasonable agreement with experimental data, because C_2H_4 is the only intermediate hydrocarbon fragment assumed in this mechanism. All of the four mechanisms explained the increased carbon monoxide concentration with increase in equivalence ratio, but no quantitative comparison could be made.

Summary

Flametube combustor experiments were conducted at an inlet pressure of 10 atm and inlet temperatures of 1000 to 1100 °F, and equivalence ratios ranging from 0.4 to 0.6. Calculated results from the proposed five-step mechanism indicated that our semiglobal simplified mechanism approach shows promise for use in combustor modeling codes. Work is continuing on improving the mechanism and testing it over a wider range of experimental conditions.

References

1. Westbrook, C.K., and Pittj, W.J., "A Comprehensive Chemical Kinetic Reaction Mechanism for Oxidation and Pyrolysis of Propane and Propane," Combustion Science and Technology, Vol. 37, Nos. 3-4, 1984, pp. 117-152.
2. Jachimowski, C.J., "Chemical Kinetic Reaction Mechanism for the Combustion of Propane," Combustion and Flame, Vol. 55, Feb. 1984, pp. 213-224.
3. Freeman, G., and Lefebvre, A.H., "Spontaneous Ignition Characteristics of Gaseous Hydrocarbon—Air Mixtures," Combustion and Flame, Vol. 58, Nov. 1984, pp. 153-162.
4. Edelman, P.B., and Fortune, O.F., "A Quasi-Global Chemical Kinetic Model for the Finite Rate Combustion of Hydrocarbon Fuels with Application to Turbulent Burning and Mixing in Hypersonic Engines and Nozzles," AIAA Paper 69-86, Jan. 1969.
5. Hautman, D.J., Dryer, F.L., Schug, K.P., and Glassman, I., "A Multiple-Step Overall Kinetic Mechanism for the Oxidation of Hydrocarbons," Combustion Science and Technology, Vol. 25, 1981, pp. 219-235.
6. Kiehne, T.M., Matthews, R.D., and Wilson, D.E., "An Eight-Step Kinetics Mechanism for High Temperature Propane Flames," Combustion Science and Technology, Vol. 54, 1987, pp. 1-23.

7. Private communication with Dr. L. Pfefferle, Yale University, CT., 1992.
8. Miller, J.A., and Bowman, C.T., "Mechanism and Modeling of Nitrogen Chemistry in Combustion," Progress in Energy and Combustion Science, Vol. 15, No. 4, 1989, p. 287.
9. Lai, M.C., "Experimental Study of Breakup and Atomization Characteristics of Fuel Jet Inside a Venturi Tube," Presented at the Central States Technical Meeting of the Combustion Institute, Columbus, OH, Apr. 26-28, 1992.
10. Deur, J.M., Kundu, K.P., and Hguyen, H.L., "Applied Analytical Combustion/Emissions Research at the NASA Lewis Research Center—A Progress Report," AIAA Paper 92-3338, July 1992.
11. Lee, C.M., Ratvasky, W., Locke, R., and Ghorashi, B., "Effect of Fuel-Air Mixing Upon NO_x Emissions for a Lean Premixed Prevaporized Combustion System," to be published as NASA TM , 1993.
12. Radhakrishnan, K., "Decoupled Direct Method for Sensitivity Analysis in Combustion Kinetics," NASA CR-179636, 1987.

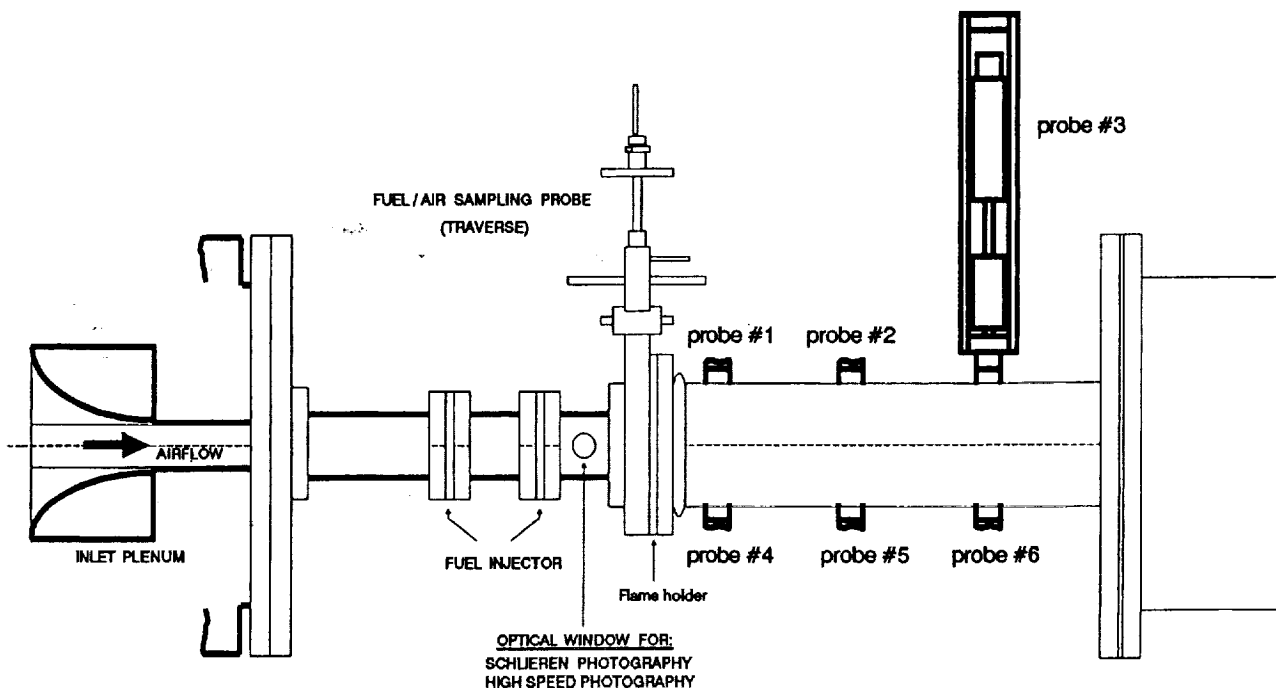


Figure 1.—High pressure and temperature flame tube combustor rig.

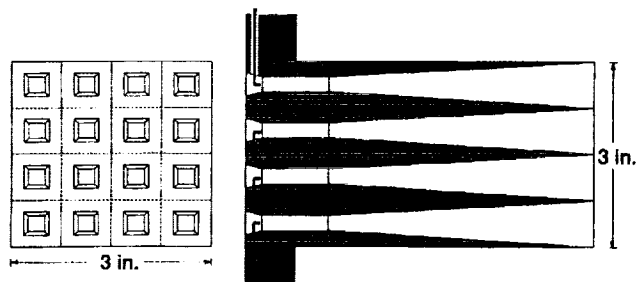
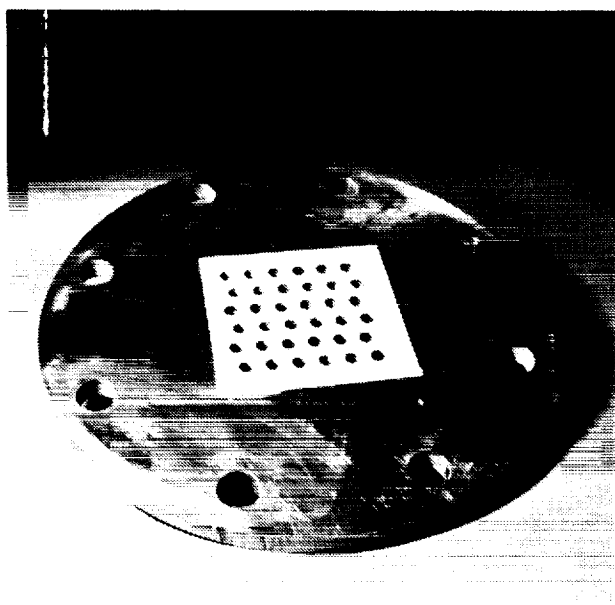


Figure 2.—Multiple tube fuel injector.

ORIGINAL PAGE
BLACK AND WHITE PHOTOGRAPH



C-91-03455

Figure 3.—Uncooled flame holder.

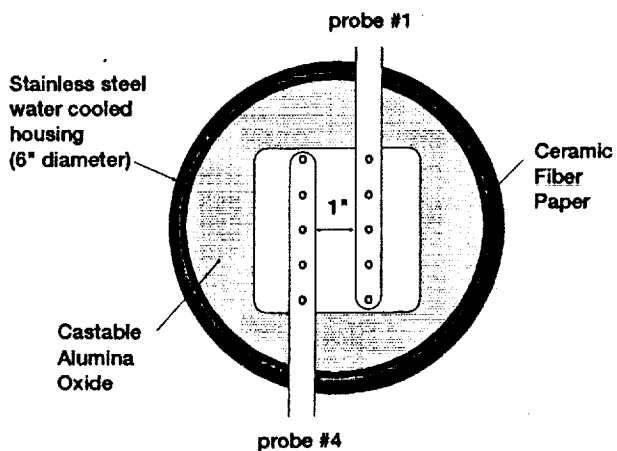
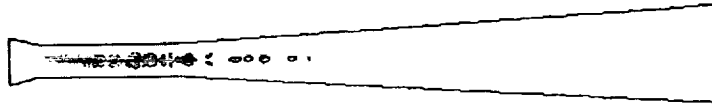


Figure 4.—Flame tube cross section and sampling probes.

1. 00000
2. 00000
3. 00000
4. 00000
5. 00000
6. 00000
7. 00000
8. 00000
9. 00000
10. 00000
11. 00000
12. 00000
13. 00000
14. 00000
15. 00000
16. 00000
17. 00000
18. 00000
19. 00000
20. 00000
21. 00000
22. 00000
23. 00000
24. 00000
25. 00000
26. 00000
27. 00000
28. 00000
29. 00000
30. 00000
31. 00000
32. 00000
33. 00000
34. 00000
35. 00000
36. 00000
37. 00000
38. 00000
39. 00000
40. 00000
41. 00000
42. 00000
43. 00000
44. 00000
45. 00000
46. 00000
47. 00000
48. 00000
49. 00000
50. 00000
51. 00000
52. 00000
53. 00000
54. 00000
55. 00000
56. 00000
57. 00000
58. 00000
59. 00000
60. 00000
61. 00000
62. 00000
63. 00000
64. 00000
65. 00000
66. 00000
67. 00000
68. 00000
69. 00000
70. 00000
71. 00000
72. 00000
73. 00000
74. 00000
75. 00000
76. 00000
77. 00000
78. 00000
79. 00000
80. 00000
81. 00000
82. 00000
83. 00000
84. 00000
85. 00000
86. 00000
87. 00000
88. 00000
89. 00000
90. 00000
91. 00000
92. 00000
93. 00000
94. 00000
95. 00000
96. 00000
97. 00000
98. 00000
99. 00000
100. 00000



1200.000
1300.000
1400.000
1500.000
1600.000
1700.000
1800.000
1900.000

Figure 5.—Jet-A droplet population contours for venturi fuel injector.

Line	Std. Dev.	Mean
A	15.36	36.10
B	32.64	65.79
C	47.26	99.44
D	49.17	102.34
E	52.57	114.00
F	50.04	127.28
G	48.42	140.49
H	42.48	122.62
I	30.43	68.73

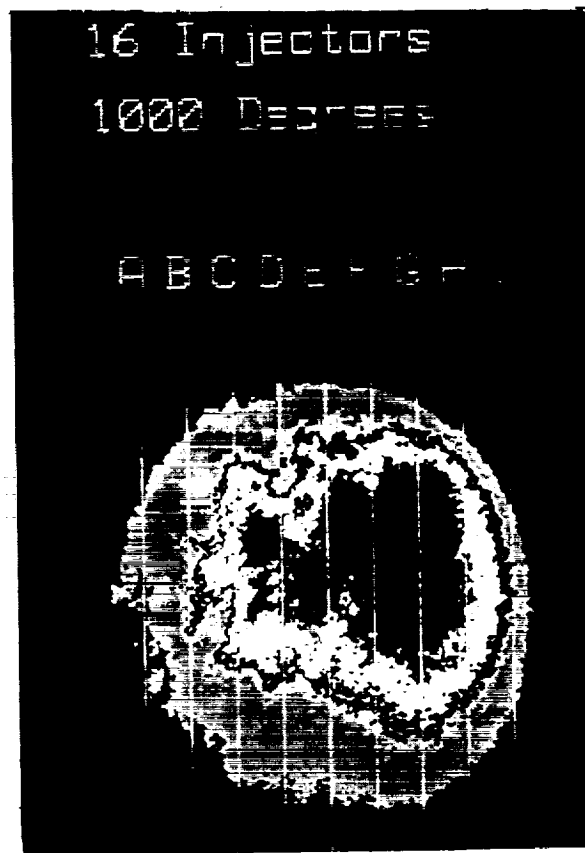


Figure 6.—Digitized flow field at premixed section.

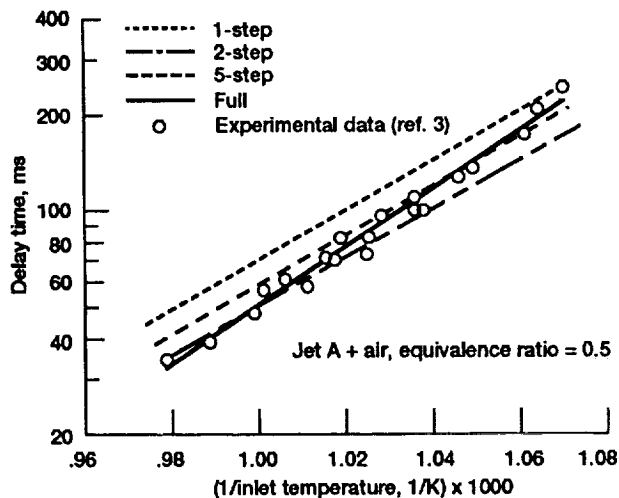


Figure 7.—Comparison of ignition delay times.

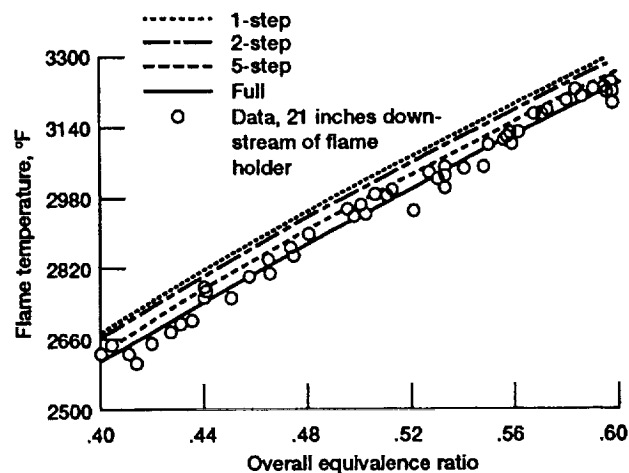


Figure 8.—Comparison of analytical & experimental flame temperatures.

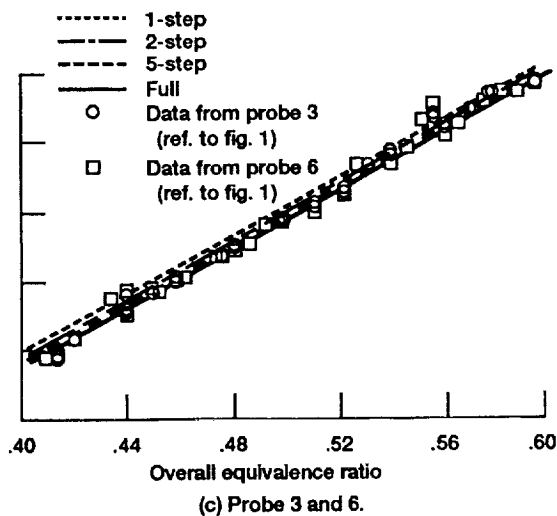
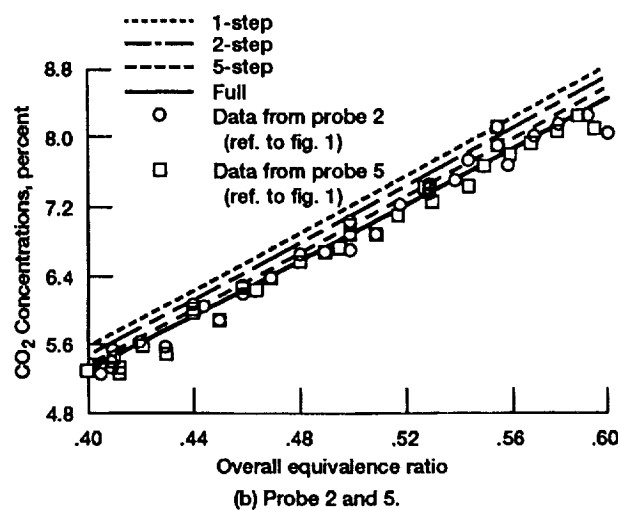
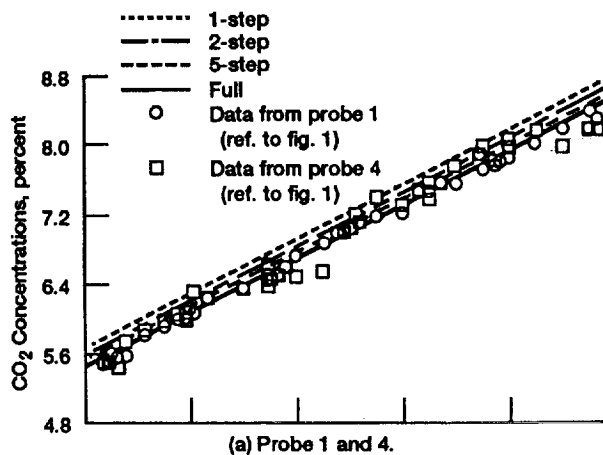
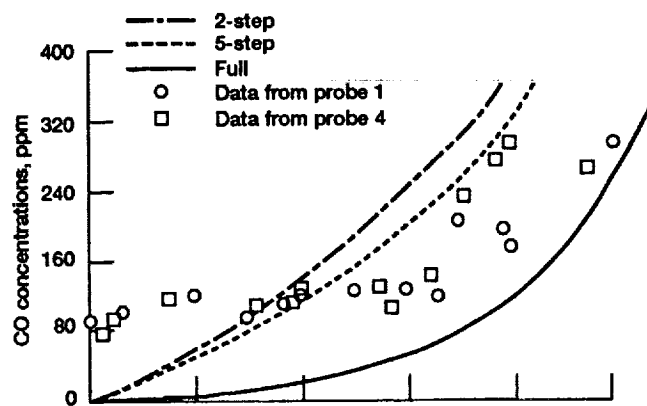
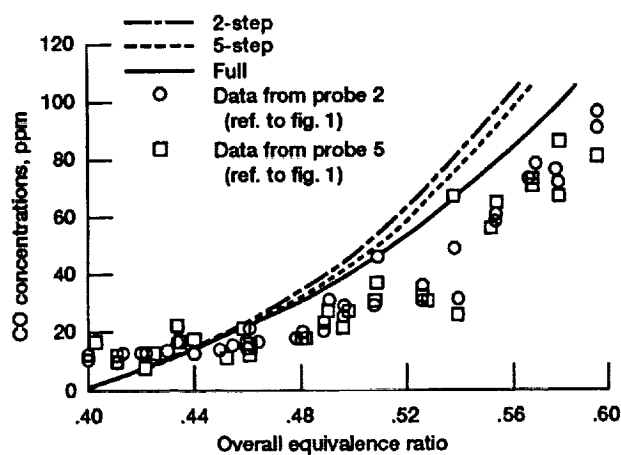


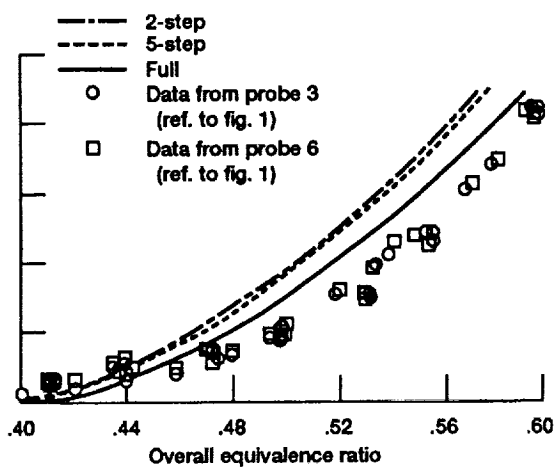
Figure 9.—Comparison of analytical & experimental CO₂ concentrations.



(a) Probe 1 and 4.



(b) Probe 2 and 5.



(c) Probe 3 and 6.

Figure 10.—Comparison of analytical & experimental CO concentrations.

REPORT DOCUMENTATION PAGE			Form Approved OMB No. 0704-0188	
Public reporting burden for this collection of information is estimated to average 1 hour per response, including the time for reviewing instructions, searching existing data sources, gathering and maintaining the data needed, and completing and reviewing the collection of information. Send comments regarding this burden estimate or any other aspect of this collection of information, including suggestions for reducing this burden, to Washington Headquarters Services, Directorate for Information Operations and Reports, 1215 Jefferson Davis Highway, Suite 1204, Arlington, VA 22202-4302, and to the Office of Management and Budget, Paperwork Reduction Project (0704-0188), Washington, DC 20503.				
1. AGENCY USE ONLY (Leave blank)		2. REPORT DATE January 1993		3. REPORT TYPE AND DATES COVERED Technical Memorandum
4. TITLE AND SUBTITLE Simplified Jet-A Kinetic Mechanism for Combustor Application			5. FUNDING NUMBERS WU-537-01-11	
6. AUTHOR(S) Chi-Ming Lee, Krishna Kundu, and Bahman Ghorashi				
7. PERFORMING ORGANIZATION NAME(S) AND ADDRESS(ES) National Aeronautics and Space Administration Lewis Research Center Cleveland, Ohio 44135-3191			8. PERFORMING ORGANIZATION REPORT NUMBER E-7457	
9. SPONSORING/MONITORING AGENCY NAMES(S) AND ADDRESS(ES) National Aeronautics and Space Administration Washington, D.C. 20546-0001			10. SPONSORING/MONITORING AGENCY REPORT NUMBER NASA TM-105940 AIAA-93-0021	
11. SUPPLEMENTARY NOTES Prepared for the 31st Aerospace Sciences Meeting sponsored by the American Institute of Aeronautics and Astronautics, Reno, Nevada, January 11-14, 1993. Chi-Ming Lee and Krishna Kundu, NASA Lewis Research Center; Bahman Ghorashi, Cleveland State University, Cleveland, Ohio. Responsible person, Chi-Ming Lee, (216) 433-3413.				
12a. DISTRIBUTION/AVAILABILITY STATEMENT Unclassified - Unlimited Subject Category 25			12b. DISTRIBUTION CODE	
13. ABSTRACT (Maximum 200 words) Successful modeling of combustion and emissions in gas turbine engine combustors requires an adequate description of the reaction mechanism. For hydrocarbon oxidation, detailed mechanisms are only available for the simplest types of hydrocarbons such as methane, ethane, acetylene, and propane. ^{1,2} These detailed mechanisms contain a large number of chemical species participating simultaneously in many elementary kinetic steps. Current computational fluid dynamic (CFD) models must include fuel vaporization, fuel-air mixing, chemical reactions, and complicated boundary geometries. To simulate these conditions a very sophisticated computer model is required, which requires large computer memory capacity and long run times. Therefore, gas turbine combustion modeling has frequently been simplified by using global reaction mechanisms, which can predict only the quantities of interest: heat release rates, flame temperature, and emissions. Jet fuels are wide-boiling-range hydrocarbons with ranges extending through those of gasoline and kerosene. These fuels are chemically complex, often containing more than 300 components. Jet fuel typically can be characterized as containing 75 vol % paraffin compounds and 25 vol % aromatic compounds. A five-step Jet-A fuel mechanism which involves pyrolysis and subsequent oxidation of paraffin and aromatic compounds is presented here. This mechanism is verified by comparing with Jet-A fuel ignition delay time experimental data, and species concentrations obtained from flametube experiments. This five-step mechanism appears to be better than the current one- and two-step mechanisms.				
14. SUBJECT TERMS Jet fuels; Kinetic mechanism; Combustion			15. NUMBER OF PAGES 12	
			16. PRICE CODE A03	
17. SECURITY CLASSIFICATION OF REPORT Unclassified	18. SECURITY CLASSIFICATION OF THIS PAGE Unclassified	19. SECURITY CLASSIFICATION OF ABSTRACT Unclassified	20. LIMITATION OF ABSTRACT	